Asian Journal of Chemistry; Vol. 35, No. 11 (2023), 2708-2714

ASIAN JOURNAL OF CHEMISTRY

https://doi.org/10.14233/ajchem.2023.30245

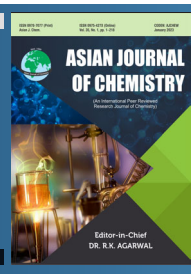

Synthesis and Characterization of Cresol based Benzoxazine–Polyurethane Copolymer for Anti-corrosion Performance of Mild Steel

C. USHA*, M. SIVARAJU and P. SHANMUGASUNDARAM

PG & Research Department of Chemistry, Thiruvalluvar Governement Arts College (Affiliated to Periyar University), Rasipuram, Namakkal-637401, India

*Corresponding author: E-mail: tkr_jai@hotmail.com

Received: 13 August 2023; *Accepted*: 17 September 2023; *Published online*: 31 October 2023; AJC-21426

The cresol based polymeric materials were synthesized by using benzoxazine and polyurethanes as copolymer. Three copolymers were synthesized by varying the quantity of polyurethane content and studied their corrosion inhibition properties. The synthesized monomer, which has cresol as the center core was characterized by the NMR, FT-IR and UV-visible spectroscopic methods. All the obtained benzoxazine polymers were also analyzed by the FT-IR and UV-visible spectroscopy. In relation to corrosion inhibition studies, Tafel and impedance experiments were conducted, revealing that benzoxazine-polymer with a higher polyurethane content has improved anti-corrosive characteristics. Additionally, the physical properties of the materials were also studied such as water absorption and gel content studies. Furthermore, the density functional theory calculation was also carried out for the monomer, which explores the better results that are matched with the other experimental studies.

Keywords: Cresol, Benzoxazine, Polyurethane, Co-polymer, Corrosion inhibition, DFT.

INTRODUCTION

Mild steel (MS) is widely used in major sectors due to its favourable material characteristics and cost-effectiveness. Because of its low cost, desirable comprehensive mechanical qualities and wear resistance, mild steels are commonly employed as the workpieces in the production and processing of aluminum goods [1,2]. The economies of industrialized countries are affected by mild steel corrosion exposure, which is estimated to cost more than 1.8 trillion USD annually globally [3]. Additionally, corrosion on mild steel does have a detrimental effect on human health, causing side effects including inflammation and allergic reactions because biomaterials are constantly being pushed to their limits by biological fluids [4,5]. Therefore, the scientific community faces a greater challenge in decreasing corrosion on mild steel, which is why researchers are more interested in organic coatings that might shield the metallic surface from corrosion [6-9]. Due to their process ability, great chemical resistance, high crosslinking density and strong adhesion/affinity to substrates, epoxy based resins have been employed extensively in recent years as a coating material to restrict the corrosion of mild steel [10,11]. However, some disadvantages, such as greater water uptake and a highly hydro-scopic character, also serve as a barrier to their use in particle applications [12,13].

Unlike epoxides, phenolic resin provides an opportunity for those capable of doing heat treatment to easily manufacture polymers [14]. Additionally, this type of polymer investigates highly important characteristics including a less hydrophilic nature, almost no shrinkage, low surface free energy and dielectric properties [15,16]. A new kind of thermosetting phenolic resin known as polybenzoxazine also demonstrates desired qualities like excellent heat and chemical resistance, high char yield and an extended shelf life [17]. The Mannich condensation reaction between a primary amine, formaldehyde and phenol has also been used to synthesize the monomers [18]. It suffers from its anti-corrosive efficiencies, such as high curing temperature and brittleness, although having many benefits due to its restrictions [19,20]. The benzoxazine-based polymers might be functionalized to address this and polyurethane is one of the best materials with a high degree of mechanical stability [21,22]. So, the idea of combining polyurethane and

benzoxazine to create a polymeric material with potential for fascinating properties has emerged. As a consequence of this, the anti-corrosive properties of the benzoxazine-polyurethane copolymer have been explored. By changing the benzoxazine and polyurethane ratios 100:60, 100:80 and 100:100, three distinct polymers have been described. The NMR, FT-IR and UV-visible spectroscopy were used to characterize the synthesized monomer and materials were inspected for corrosion investigations.

EXPERIMENTAL

For recording FT-IR spectra, Thermo-Scientific Nicolet iS50 FT-IR spectrometer was used. For proton and carbon spectra, Bruker 500 MHz and 125 MHz NMR was used and samples were dissolved in $CDCl_3$ or DMSO-d_6. A Labman LMSP UV-1200 UV-Vis spectrometer was used to record UV-Vis spectrum. On 2 cm × 5 cm pre-coated silica gel 60 F_{254} plates of a thickness of 0.25 mm, the progress and completion of reactions was monitored by TLC. The TLCs were visualized using UV 254-365 nm and/or iodine. Polarization measurements were performed in a conventional three-electrode cell. The Ag/AgCl and the platinum electrode were used as reference and counter electrodes, respectively. The potentiostatic polarization measurement was carried out using electrochemical workstation Biologic SP 300 model. The energy of the acceleration beam was employed at 20 keV. The surface analysis was performed on a GOM plastic microscope 100x object lens.

Synthesis of monomer: To synthesize a monomer, *o*-cresol (1 g, 6.572 mmol), glycine ethyl ester·HCl (6.572 mmol) and paraformaldehyde (0.414 g, 13.802) were dissolved in chloroform (20 mL) and refluxed for 24 h. Meanwhile, the progress of the reaction was monitored by TLC. After completion of the reaction, the reaction mixture was extracted with chloroform (150 mL) and washed with 0.5 N NaOH (100 mL), washed with water (100 mL) and brine solution (100 mL) to remove the water-soluble impurities. The obtained organic layer was separated out and dried over an anhydrous sodium sulphate. This chloroform evaporated under reduced pressure yielded benzoxazine monomer (**Scheme-I**). This obtained monomer was used for the preparation of the coating material with poly-urethane as polymeric contents.

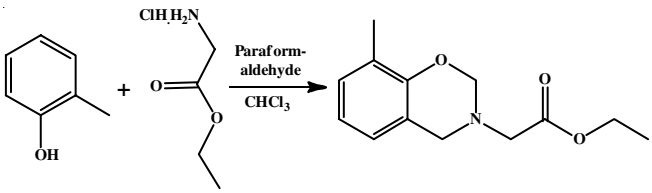

Scheme-I: Synthesis of cresol based monomer

Synthesis of cresol benzoxazine (Cbzs) anti-corrosive agents: Before coating, the mild steel (MS) substrates were mechanically blasted to Sa 2.1/2 and washed ultrasonically in acetone. The polymer was coated on the MS plate by dip coating and thermal curing techniques. The monomer (Cbz) was first dissolved in a mixture of solvents (7:3 1,4-dioxane/toluene) and then various equivalent amounts of the isocyanate hardener were added to it, such as 100:60 (Cbz-PU 60), 100:80 (Cbz-PU 80) and 100:100 (Cbz-PU 100). The MS plate was then dipped for 1 min in the Cbz-PU solution and then removed from it at a speed of 100 mm/min. After being left at room temperature overnight, Cbz-PU coated MS samples were dried in a vacuum for 1 h at 100 ºC, removing the solvent molecules. This specimen was then thermally treated for 3 h at 180 ºC.

Water absorption studies: Water absorption of all cured coating samples was performed as per ASTM D570. These samples were further dried at 80 ºC in an oven under vacuum condition then immersed in water at room temperature for a day. After that the absorbed water was removed from the samples and stained with tissue paper then weighed. The percentage of water absorption was calculated by using following equation:

$$\text{Water absorption } (\%) = \frac{W_a - W_b}{W_b} \times 100$$

where W_a = weight of the cured sample after removal the exposure to water absorption; W_b = weight of the cured sample before removal the exposure to water absorption.

Gel content studies: The total gel content of the cured coating sample was determined by weighing the bare coated sample accurately and extracted in xylene solvent for 24 h at room temperature. Then cured coating samples were dried in the oven under vacuum environment. Gel content of coated samples was calculated by the following equation:

$$\text{Gel content } (\%) = \frac{W_a}{W_b} \times 100$$

where W_a and W_b are the weight of cured coating samples after and before the extraction, respectively.

Computational calculations: The monomer's frontiers molecular orbitals (FMO) molecular orbitals (FMO) of the monomer were investigated using density functional theory (DFT). The software used for these calculations is the Gaussian 09W software. For the monomer's structural optimization, the B3LYP/6-311G basis set was applied [23]. The Gauss view software was used for various further process such as three-dimensional visualization including FMO, electron clouds identification on the compound, molecular electrostatic potential (MEP).

RESULTS AND DISCUSSION

The cresol based benzoxazine monomer (Cbz) was synthesized from *o*-cresol by Mannich condensation method. The glycine ethyl ester was used as a amine precursor and paraformaldehyde is used as cyclizing agent. The synthesized Cbz was extracted from the reaction mixture and characterized by spectroscopic technique. The synthesized Cbz was polymerized with different ratio of poly urethane after mild steel (MS) plate coating. The synthetic route for Cbz is represented in **Scheme-I** and polymerization is represented in **Scheme-II**.

FT-IR studies: Each functional group in an organic molecule has its unique vibrational frequency, which is legitimate information provided by FT-IR spectroscopy. The functional groups of ester, cyclic amine and cyclic ether are present in the synthesized monomer and can be strictly recognized by FT-IR

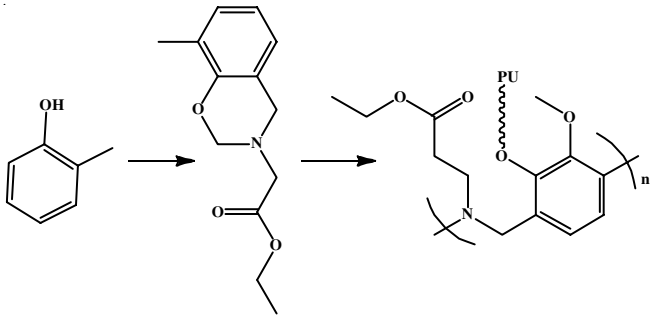

Scheme-II: Pictorial representation of benzoxazine-polyureathane co-polymer

spectroscopy. The molecule exhibits a series of peaks between 2984 and 2853 cm^{-1}, which correspond to aromatic stretching vibrations and a prominent peak at 1679 cm^{-1}, which corresponds to the ester carbonyl stretching vibration (Fig. 1). The absence of a distinctive peak in the amine NH vibrations amplifies the presence of the *tertiary* amine in the compound. Additionally, there is a strong peak at 1197 cm^{-1} that is linked to the cyclic amine functional group's C-N stretching vibration. Peaks at 1266, 1297 and 1023 cm^{-1} correspond to the asymmetric and symmetric stretching vibrations of the C-O-C bond, respectively. The existence of an *ortho*-substituted epoxy group was revealed by a strong signal at 750 cm^{-1} and a further peak at 1484 cm^{-1} strongly confirms the presence of a tri-substituted benzene ring that has been fused with an oxazine ring. This study is highly confirmed that the synthesized monomer having respective functional group particularly oxazine ring fused with aromatic group [24]. These matching peaks were likewise found for the polymeric composites and additional noteworthy peaks that correlate to the vibrations of polyurethane were also seen. For instance, the -NH- and $-CH_2$ stretching vibrations are responsible for the weak boarded peaks that were obtained at 3378 and 2910 cm^{-1}, respectively. A modest peak at 1731 cm^{-1} was observed, confirming the -C=O group's presence in the polyurethane unit. In addition, a series of strong peaks at 1524 and 1119 cm^{-1} that are related to the stretching vibrations of the C-N and C-O-C bonds, respectively [25]. In this way, the presence of polyurethane unit in the synthetic composites is confirmed.

NMR studies: The proton and carbon NMR analysis was used to describe the synthesized Cbz. The lack of a broad signal in the proton NMR suggests that the reactant ($-NH_2$) does not contain a labile proton, which encourages the formation of the alicyclic ring. Additionally, three distinctive peaks of aliphatic $-CH_2$ groups were found at 3.42, 3.74 and 4.89 ppm, further supporting the formation of the oxazine ring. The methyl group linked to the benzene ring and the ethyl group of the ester is represented by other distinctive peaks at 2.15, 4.14 and 1.23 ppm, respectively. At 6.82 ppm, three aromatic protons are found and revealed as three protons after integration. Similar to this, the carbon NMR also exhibits important peaks at δ 82.7, 52.4 and 50.1 ppm that point to the formation of the benzoxazine ring and significant peaks at δ 170.6 ppm that are attributable to the carbonyl carbon.

UV-visible studies: The UV-visible spectroscopy investigations used the synthesized Cbz. Because of this, 1,4-dioxane was used as a solvent to dissolve the monomer and the spectra was captured at ambient temperature. The Cbz exhibits two peaks at 330 nm and 286 nm, with the first peak being obtained to broaden and the latter peak being obtained as a high absorbance peak as shown in Fig. 2. These two peaks are associated with the n-π* and π-π* electronic transitions of the compound. Similarly, polyurethane coupled materials also were studied and except Cbz-PU100 other, three samples shows the two major band at 280 nm and 335 nm, which is almost resembles with Cbz band. But, sample Cbz-PU100 had spectrum with splitting of lower region band in to two soft edged band at 263 and 280 nm in addition to that respective π-π* transition band also observed at 335 nm similar to other samples. These results indicates that large amount of polyurethane has influences the n-π* transition thus shows its own behaviours also. Hence, this dominance of the polyurethane in the Cbz-PU100 could be helpful for the application process.

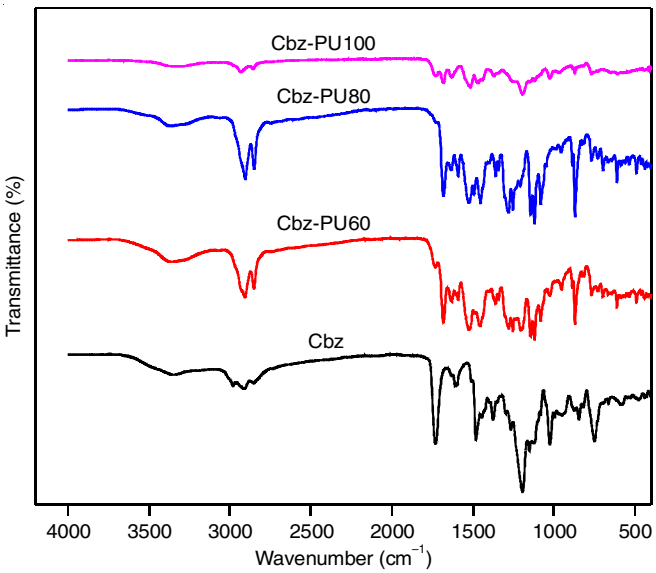

Fig. 1. FT-IR spectra of the monomer and polymeric composites

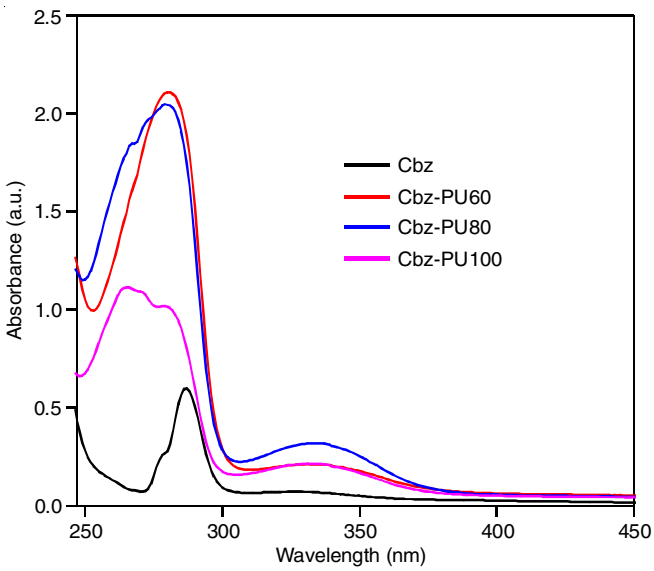

Fig. 2. UV-visible spectra of the monomer and polymeric composites

Corrosion studies: The obtained Tafel polarization curves are plotted together and shown in Fig. 3, from that, corrosion current and corrosion potential were calculated. The corrosion current density was calculated by superimposing a straight line along with the linear component of the cathodic or anodic curve and extrapolating it using corrosion potential. More negative E_{corr} and larger I_{corr} often indicate a faster rate of corrosion, whereas more positive E_{corr} and smaller I_{corr} indicate a slower rate of corrosion. The following equations were used to determine the corrosion rate and protection efficiency.

$$\text{Corrosion rate} = \frac{I_{corr} \times K \times EW}{\rho A}$$

$$\text{Corrosion efficiency } (\%) = \left(\frac{I_{corr(b)} - I_{corr(c)}}{I_{corr(b)}} \right) \times 100$$

where K = the corrosion rate constant (3272 mm year^{-1}); EW = equivalent weight (27.9 g); ρ = the material density (7.85 g cm^{-3} for MS) and A = the sample area (1 cm^2). The I_{corr} and $I_{corr(c)}$ were the corrosion current values in the absence and presence of the coatings, respectively [26,27]. The calculated values of E_{corr} and I_{corr} were extrapolated from the Tafel polarization curves and tabulated in Table-1. The bare metal MS shows -506.056 mV and 82.89 µA of E_{corr} and I_{corr}, respectively which clearly indicates that having highly corrosion nature. This was improved by coating with Cbz based polymer thus given -502.097 mV and 5.631 µA of E_{corr} and I_{corr}, respectively leads to less corrosive than plain metal. This corrosive nature is still get decreased by the increasing coating of polyureathane with respective to amount of urethane. The higher amount of polyurethane thus given higher E_{corr} and very lower I_{corr} *i.e.* -480.953 mV and 5.151 µA, respectively than other Cbz polymer coating that are having less amount of urethane. This studies that clearly indicates Cbz-PU100 would be restrict correction significantly rather than without coating. Based on the results, the corrosion rate also calculated and given in Table-1. This result shows that more polyurethane coated still thus shows less corrosion rate compared to the bare metal still. Moreover, the corrosion efficiency also gives valid results of the effect of coating; all the coated samples thus show almost equal corrosion efficacy among them sample Cbz-PU100 showing higher efficiency rather than the others.

TABLE-1
RESULTS OF ELECTROCHEMICAL CORROSION MEASUREMENTS FOR DIFFERENT SAMPLES IN 3.5 wt.% NaCl SOLUTIONS

Compounds	E_{corr} (mv)	I_{corr} (µA)	Corrosion rate (mmpy)	Corrosion efficiency (%)
Blank	-506.056	82.87	963706.87	0
Cbz-PU60	-502.097	5.631	65483.69	93.20
Cbz-PU80	-494.998	5.289	61506.52	93.61
Cbz-PU100	-480.953	5.151	59901.70	93.78

It is well-known that studies on diffusion of water in to polymeric corrosion material is important things which can depends on the branches and cross-linkage density of the polymeric materials. The functionality of binder during the coating, which is decided the density of the cross or branch density that can provide better hydrogen bonding with materials [5]. Henceforth, here Cbz-PU100 having more amount of urethane, which would reduce the porosity meantime it increases restrictions thus, Cbz-PU100 material could be achieve lower water diffusion and higher gel formation. This has been verified by two experimental methods *viz*. the assessment of gel content and water diffusion studies. The results of both experiments are showed in Figs. 4 and 5, respectively. All the materials absorbed 2.11% of the water molecules hence, it would make more corrosion to the metal in fastest way thus was observed in the Tafel plot experiment also. Similarly, amount of the gel content in the Cbz also very less that suggests that absence of any cross-linkage and branches leads to more water absorption. Whereas, increasing content of the urethane have creates more cross and branches linkage with Cbz, which blocks the water absorption by reducing the porosity of the Cbz. Finally, the higher concentration of urethane Cbz-PU100 thus show less than 1% of the water absorption and the gel formation was also increased greatly (> 95%). The obtained results suggested that high concentrated urethane, which can protect the still plant from the corrosion in the better way.

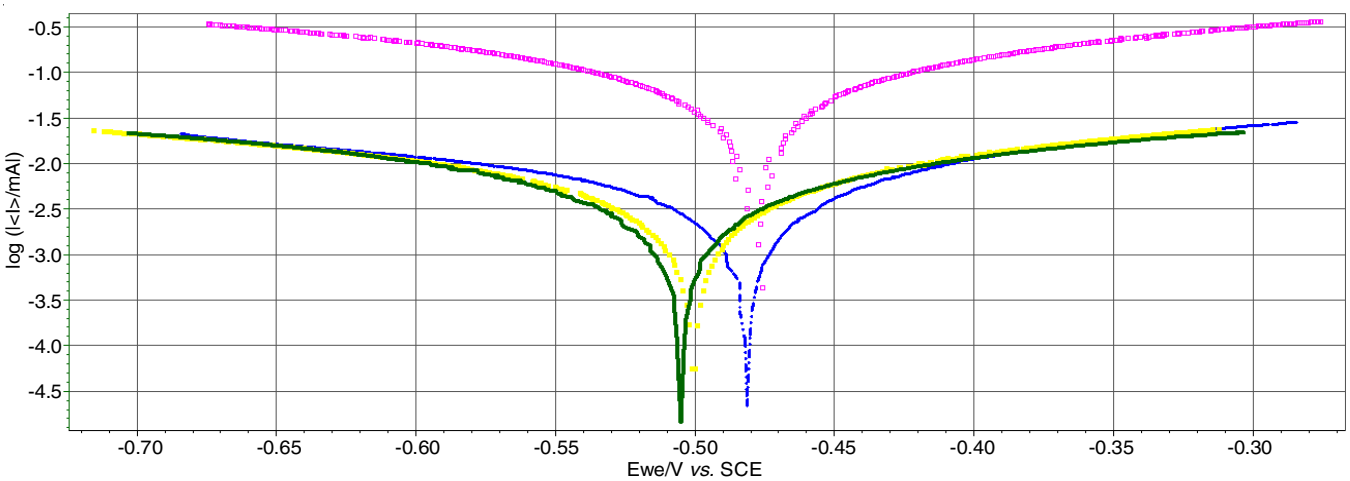

Fig. 3. Tafel curves for different electrodes measured in 3.5 wt% NaCl aqueous solution, (1) Bare MS; (2) Cbz-PU100, (3) Cbz-PU80 and (4) Cbz-PU60

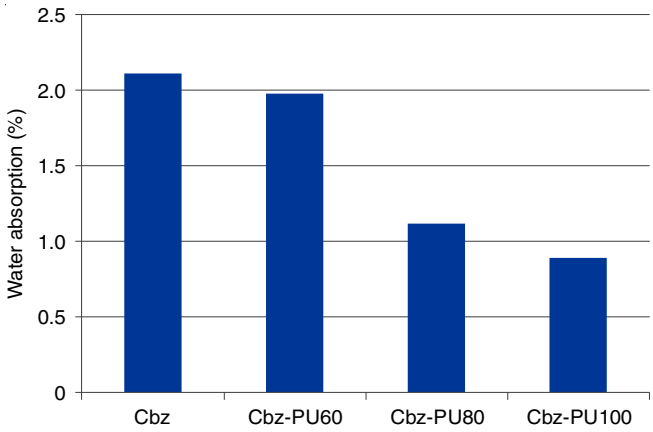

Fig. 4. Water absorption studies of the Cbz with different PU combinations

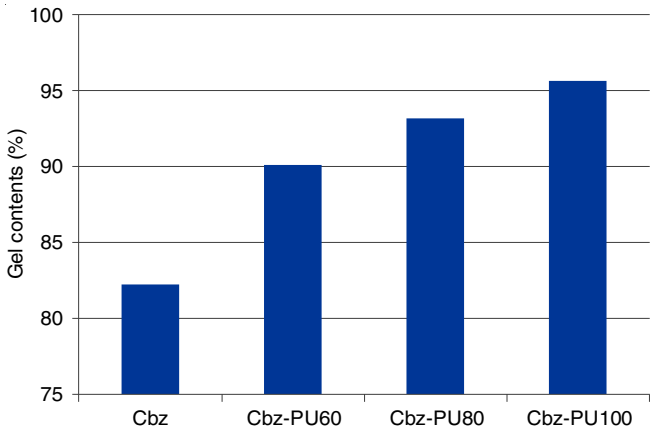

Fig. 5. Gel content studies of the Cbz with different PU combinations

The polymer coated and uncoated mild still plate was studied by the EIS Bode plots and data were plotted. Here, EIS data for all polymeric materials coated plates were carried out by using simple equivalent electric circuit model. This model includes several elements such as resistor R_s which related to the resistance of the solution, a constant phase element to the capacitance of the electrical double layer that occurred between metal and liquid surface and a resistor R_{ct} related to the polymer as we used for the coating and resistance at the metal–polymer interface or to the polymer–solution resistance (Fig. 6). The MS plate's polymeric covering greatly raises the blank's R_{ct} from 261 Ω cm^2, which is quite low. The maximum R_{ct} value was obtained for Cbz-PU60, which was 29793 Ω cm^2, while Cbz-PU100 had a R_{ct} value of 4899 Ω cm^2, which is raised by increasing polyurethane content (Table-2). These findings suggest that adding extra polyurethane can provide corrosion-resistant barriers.

$$\text{Inhibition efficiency (\%)} = \frac{R_{ct(c)} - R_{ct(b)}}{R_{ct(c)}} \times 100$$

where $R_{ct\,(c)}$ = charge transfer resistance with coating and $R_{ct\,(b)}$ = charge transfer resistance without coating [6]. The obtained results that greatly supported to the previous studies and more content of the polyurethane sample (BP1) having more corrosion inhibition capability that almost reached to 100%. Finally, all studies that proven that need for the polyurethane materials and provides more crosslink structure that creates hydrophobic nature and shows high resistance to the corrosion.

TABLE-2
ELECTROCHEMICAL PARAMETERS EXTRACTED FROM THE EIS BLONDE CURVES

Compounds	R_{ct} (ohm)	Inhibition efficiency (%)
Blank	261	0
Cbz-PU100	4899	94.67
Cbz-PU80	13125	98.01
Cbz-PU100	29793	99.12

Microscopic optical studies: A visible anti-corrosive efficacy might be obtained by analyzing microscopic optical image investigations of the coated polymer's impacts. The impact of the polymer material concentration on the coating materials is shown in Fig. 7. The whole morphological damage with a dark red colour is revealed as a result of the bare MS yet getting impacted aggressively. Investigates the fact that polymeric composites have been coated despite mild yet inadequate anti-corrosive properties. Even though the MS is coated with 60% loaded material, its shape is almost completely preserved. However, the dark red colour indicates that it lacks

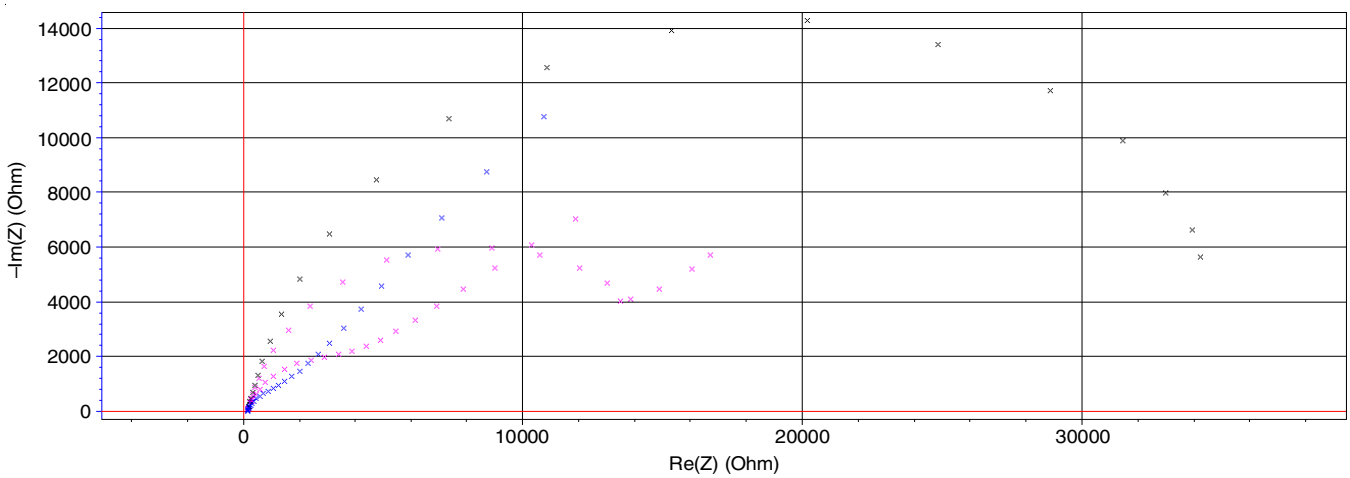

Fig. 6. EIS blonde spectra of mild still and coated MS with Cbz-PU100, Cbz-PU80 and Cbz-PU60 after immersion in 3.5 wt% NaCl solution for different periods of time

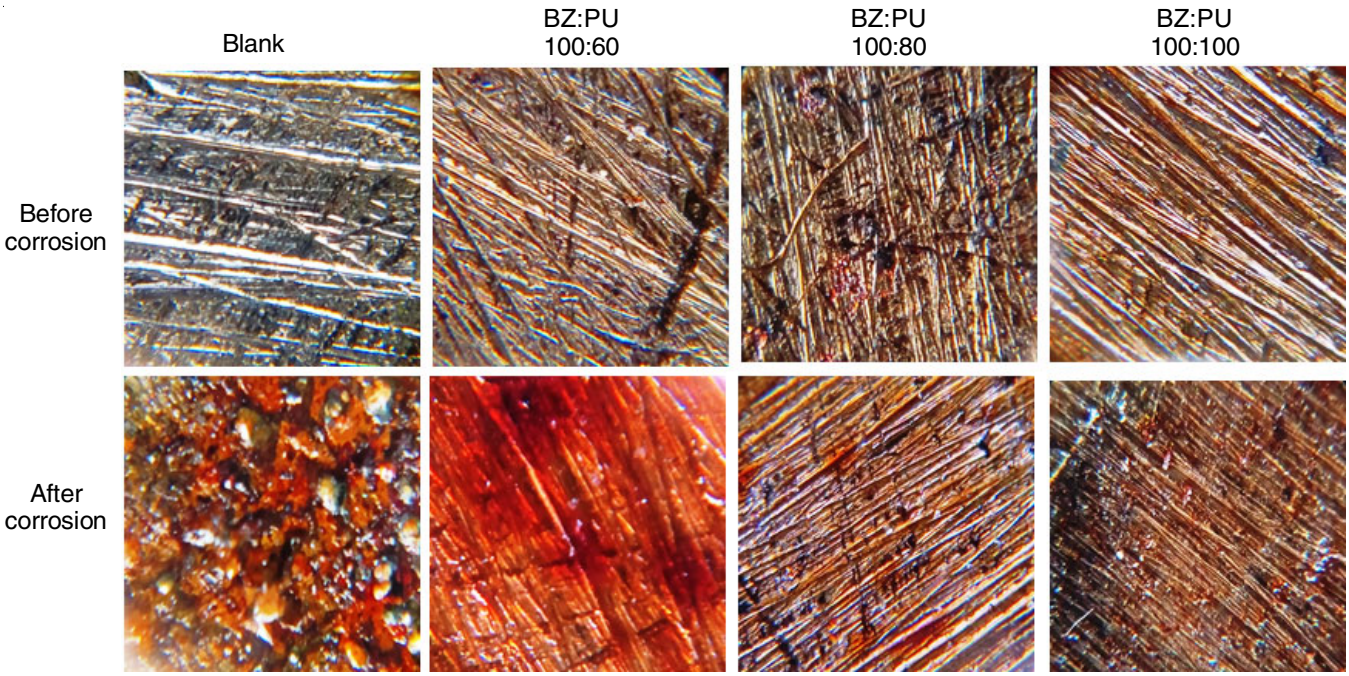

Fig. 7. Optical images of the bare and with coated mild still plates before and after corrosion

anti-corrosive capabilities. Following the corrosive, 80% polyurethane materials are applied to the MS to change the colour. Furthermore, the higher polyurethane content (Cbz-PU100) that doesn't even alter the colour of the MS surfaces effectively quenched corrosion. Therefore, there is a strong recommendation that more polyurethane incorporates components with higher resistivity to corrosion given that these optical imaging studies also have an excellent line-up with earlier corrosive experiments.

DFT analysis: DFT analysis is a computational method that can be used to find out the electronic distribution on the molecule at ground state and excited states which are used for the various research fields [28-30]. Fig. 8 shows the monomer's HOMO and LUMO, which were obtained from the DFT analysis.

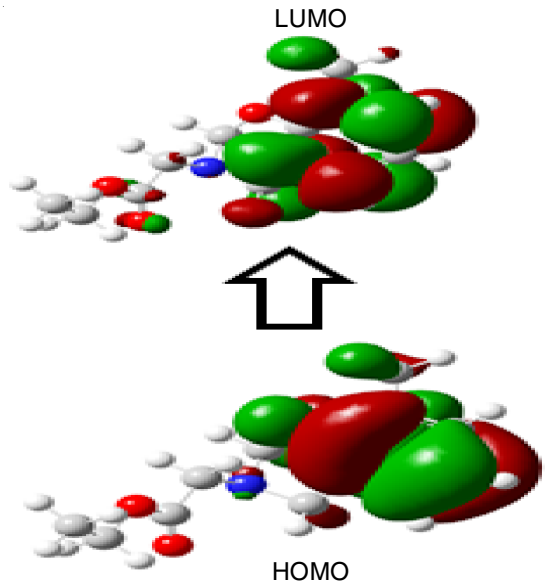

Fig. 8. Molecular orbitals of Cbz

Thus, it is evident from the molecules' electron distribution that benzoxazine moiety behaves as both HOMO and LUMO. However, HOMO exhibits a dense electron cloud, whereas LUMO exhibits a little weaker electron cloud than HOMO. These findings demonstrate that benzoxazine mostly behaves as HOMO as opposed to LUMO. A minor electronic cloud was seen at the carbonyl functional group at LUMO; however, the ester portion of the monomer has no appreciable electron density at HOMO.

Molecular electrostatic potential (MEP): The data derived from this study, which are processed by the reliable quantum chemical method. Results could help largely and used to understand and forecast of the chemical reactivity of the molecules [31]. The optimized structure of the monomer was used to find out the positive and negative potential of the molecule. This is the easiest way to predict the potential of molecules *via* colours. The more negative potential region could show red colour whereas more positive region could appear in as blue colour. The neutral region always appeared in the green colour. In this we can easily find out the molecule's potentials [32]. In the monomer's molecular potential images are shown in Fig. 9. Its seems that red colour spotted on the oxygen surfaces in particular ester carbonyl group having red colour whereas benzoxazine oxygen shows slight red colour. A green colour also finds on the nitrogen surface whereas no other significance colours are found thus hetero atom had crucial role which possessing an visible colour changes on its surface. The negative and positive regions forms the strong interactions with metal surface.

Conclusion

The present research described a novel polymeric material having polyurethane and benzoxazine as central core unit. The synthesis involved the utilization of various polyurethane

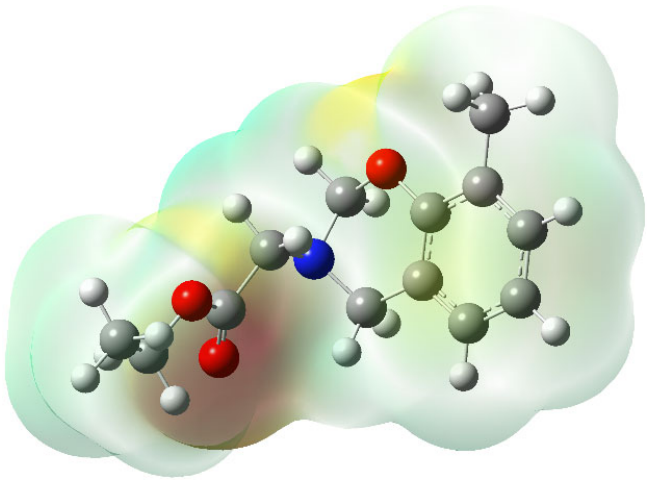

Fig. 9. Molecular electrostatic potential of Cbz

ratios, which were afterwards characterized and examined for their impact on the anti-corrosion properties. The results that exhibit outstanding corrosive behaviour were achieved using materials that contain excess amount of polyurethane. Less current intensity and higher resistivity were confirmed from the Tafel plot and EIS electrochemistry study results, which strongly hinder the mild steel (MS) electrochemical property that the coated materials experience. The results of investigations on water absorption and gel content were also in good accord with those from electrochemistry. The best anti-corrosive activity of the materials was also confirmed by the visible photographs of the corrosion activity of each material. As a result, Cbz-PU100, one of the synthesized materials, maybe a highly promising material with the potential for being corrosion resistant, opening the door to the prospect of expanding uses in future.

CONFLICT OF INTEREST

The authors declare that there is no conflict of interests regarding the publication of this article.

REFERENCES

1. L.R.V. Kotzebue, J.R. de Oliveira, J.B. da Silva, S.E. Mazzetto, H. Ishida and D. Lomonaco, *ACS Sustain. Chem. Eng.*, **6**, 5485 (2018); https://doi.org/10.1021/acssuschemeng.8b00340
2. X. Lu, Y. Liu, C. Zhou, W. Zhang and Z. Xin, *RSC Adv.*, **6**, 5805 (2016); https://doi.org/10.1039/C5RA22980D
3. G. Schmitt, M. Schütze, G.F. Hays, W. Burns, E. Han, A. Pourbaix and G. Jacobson, *FHWA-RD*, **01**, 1 (2009).
4. R.I.M. Asri, W.S.W. Harun, M. Samykano, N.A.C. Lah, S.A.C. Ghani, F. Tarlochan and M.R. Raza, *Mater. Sci. Eng. C*, **77**, 1261 (2017); https://doi.org/10.1016/j.msec.2017.04.102
5. G.A. Phalak, D.M. Patil and S.T. Mhaske, *Eur. Polym. J.*, **88**, 93 (2017); https://doi.org/10.1016/j.eurpolymj.2016.12.030
6. C. Zhou, X. Lu, Z. Xin, J. Liu and Y. Zhang, *Prog. Org. Coat.*, **76**, 1178 (2013); https://doi.org/10.1016/j.porgcoat.2013.03.013
7. A.H. Asif, M.S. Mahajan, N. Sreeharsha, V.V. Gite, B.E. Al-Dhubiab, F. Kaliyadan, S.H. Nanjappa, G. Meravanige and D.M. Aleyadhy, *Materials*, **15**, 2308 (2022); https://doi.org/10.3390/ma15062308
8. S.A. Umoren and U.M. Eduok, *Carbohydr. Polym.*, **140**, 314 (2016); https://doi.org/10.1016/j.carbpol.2015.12.038
9. S. Sriharshitha, K. Krishnadevi, S. Devaraju, V. Srinivasadesikan and S.-L. Lee, *ACS Omega*, **5**, 33178 (2020); https://doi.org/10.1021/acsomega.0c04840
10. X. Shi, T.A. Nguyen, Z. Suo, Y. Liu and R. Avci, *Surf. Coat. Technol.*, **204**, 237 (2009); https://doi.org/10.1016/j.surfcoat.2009.06.048
11. S.-W. Kuo and W.-C. Liu, *J. Appl. Polym. Sci.*, **117**, 3121 (2010); https://doi.org/10.1002/app.32093
12. A.S. Castela and A.M. Simões, *Corros. Sci.*, **45**, 1631 (2003); https://doi.org/10.1016/S0010-938X(03)00014-3
13. W.-G. Ji, J.-M. Hu, L. Liu, J.-Q. Zhang and C.-N. Cao, *Prog. Org. Coat.*, **57**, 439 (2006); https://doi.org/10.1016/j.porgcoat.2006.09.025
14. S. Jamshidi, H. Yeganeh and S. Mehdipour-Ataei, *Polym. Adv. Technol.*, **22**, 1502 (2011); https://doi.org/10.1002/pat.1634
15. J.R. Oliveira, L.R.V. Kotzebue, D.B. Freitas, A.L.A. Mattos, A.E. da Costa Jr., S.E. Mazzetto and D. Lomonaco, *Composites B Eng.*, **194**, 108060 (2020); https://doi.org/10.1016/j.compositesb.2020.108060
16. C. Peng, Z. Wu and D. Zhou, *Compos., Part B Eng.*, **167**, 507 (2019); https://doi.org/10.1016/j.compositesb.2019.02.068
17. Y. Deng, L. Xia, G.-L. Song, Y. Zhao, Y. Zhang, Y. Xu and D. Zheng, *Compos., Part B Eng.*, **225**, 109263 (2021); https://doi.org/10.1016/j.compositesb.2021.109263
18. Y.J. Lee, S.W. Kuo, Y.C. Su, J.K. Chen, C.W. Tu and F.C. Chang, *Polymer*, **45**, 6321 (2004); https://doi.org/10.1016/j.polymer.2004.04.055
19. S. Rimdusit, T. Mongkhonsi, P. Kamonchaivanich, K. Sujirote and S. Thiptipakorn, *Polym. Eng. Sci.*, **48**, 2238 (2008); https://doi.org/10.1002/pen.21171
20. S. Rimdusit, S. Pirstpindvong, W. Tanthapanichakoon and S. Damrongsakkul, *Polym. Eng. Sci.*, **45**, 288 (2005); https://doi.org/10.1002/pen.20273
21. H. Yeganeh, M. Razavi-Nouri and M. Ghaffari, *Polym. Eng. Sci.*, **48**, 1329 (2008); https://doi.org/10.1002/pen.21098
22. H. Yeganeh, M. Razavi-Nouri and M. Ghaffari, *Polym. Adv. Technol.*, **19**, 1024 (2008); https://doi.org/10.1002/pat.1070
23. R. Kavitha, S. Nirmala, R. Nithyabalaji and R. Sribalan, *J. Mol. Struct.*, **1204**, 127508 (2020); https://doi.org/10.1016/j.molstruc.2019.127508
24. M.M. Hussein, S.A. Saafan, N.A. Salahuddin and M.K. Omar, *Appl. Phys., A Mater. Sci. Process.*, **127**, 488 (2021); https://doi.org/10.1007/s00339-021-04620-8
25. S. Caddeo, F. Baino, A.M. Ferreira, S. Sartori, G. Novajra, G. Ciardelli and C. Vitale-Brovarone, *Key Eng. Mater.*, **631**, 184 (2014); https://doi.org/10.4028/www.scientific.net/KEM.631.184
26. C. Zhou, X. Lu, Z. Xin, J. Liu and Y. Zhang, *Prog. Org. Coat.*, **76**, 1178 (2013); https://doi.org/10.1016/j.porgcoat.2013.03.013
27. D. Prasai, J.C. Tuberquia, R.R. Harl, G.K. Jennings and K.I. Bolotin, *ACS Nano*, **6**, 1102 (2012); https://doi.org/10.1021/nn203507y
28. S.S. Nishat, M.J. Hossain, F.E. Mullick, A. Kabir, S. Chowdhury, S. Islam and M. Hossain, *J. Phys. Chem. C*, **125**, 13158 (2021); https://doi.org/10.1021/acs.jpcc.1c02302
29. A. Senthil Murugan, E.R. Abel Noelson and J. Annaraj, *Inorg. Chim. Acta*, **450**, 131 (2016); https://doi.org/10.1016/j.ica.2016.04.022
30. R. Zaier, S. Hajaji, M. Kozaki and S. Ayachi, *Opt. Mater.*, **91**, 108 (2019); https://doi.org/10.1016/j.optmat.2019.03.013
31. H. Suresh, G.S. Remya and P.K. Anjalikrishna, *WIREs Comput. Mol. Sci.*, **12**, e1601 (2022); https://doi.org/10.1002/wcms.1601
32. S. Lakshminarayanan, V. Jeyasingh, K. Murugesan, N. Selvapalam and G. Dass, *J. Photochem. Photobiol.*, **6**, 100022 (2021); https://doi.org/10.1016/j.jpap.2021.100022